

Effects of Geometry on Intensity of Singular Stress Fields at the Corner of Single-Lap Joints

Yu Zhang, Nao-Aki Noda, Kentaro Takaishi

Abstract—This paper discusses effects of adhesive thickness, overlap length and material combinations on the single-lap joints strength from the point of singular stress fields. A useful method calculating the ratio of intensity of singular stress is proposed using FEM for different adhesive thickness and overlap length. It is found that the intensity of singular stress increases with increasing adhesive thickness, and decreases with increasing overlap length. The increment and decrement are different depending on material combinations between adhesive and adherent.

Keywords—Adhesive thickness, Overlap length, Intensity of singular stress, Single-lap joint

I. INTRODUCTION

WITH the increasing use of adhesive joints in various practical applications, it has been paid more and more attention to the evaluation of the adhesive joints strength by experimental and analytical methods [1-5]. Due to abrupt changes in geometry and in the elastic properties between the different materials, singular stress fields exist at the edge of interface between the adhesive and the adherent. Yuki[6], Chen[7] and Munz [8] have discussed the singular stress fields in two bonded wedges for different values of θ_1, θ_2 in Fig.1. Generally, stress singularity fields are approximately expressed by the following equation[9]:

$$\sigma_{ij} \propto \frac{K_{ij}}{r^\lambda} \quad (r \rightarrow 0) \quad (1)$$

Where σ_{ij} is the stress component, r is the distance from the singular point, K_{ij} is the stress intensity factor, and λ is the order of stress singularity. The order of stress singularity λ can be imaginary number, real number, or two real roots with different θ_1, θ_2 and material combinations.

The characterization of the singular stress field is fundamental if the initiation of failure (an initial crack or localized damage whose propagation implies the complete failure of the joint) can be assumed to occur due to that singular stress field. However, few evaluations of joints strength are based on the

singularity stress fields. Hattori[10],[11] proposed an evaluation method for the strength behavior of adhesively bonded joints at a singular point using the intensity of stress singularity K and the order of stress singularity λ . However, stress singularity fields of a bonded interface are very complex, and the stress fields of adhesive joints cannot be formulated by constant singularity parameters K and λ , because they are affected by the geometry and loading conditions of adhesive joints. Imanaka [9] and Barros [12] proposed methods to determine singularity parameters of single lap-joints. However, these methods are only limited to a kind of adhesive joint geometry.

In this paper, therefore, the intensity of singular stress fields of the single lap joint will be discussed, and the effect of geometry and material combinations on the intensity will be clearly discussed.

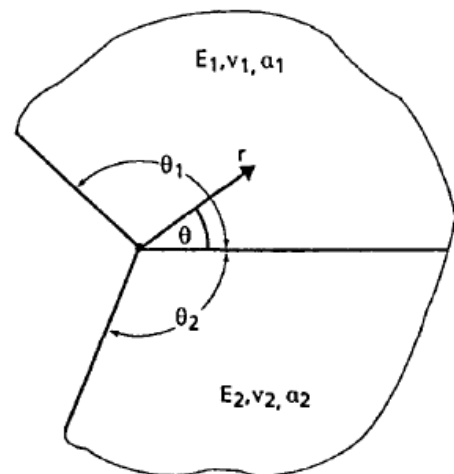


Fig.1 The Bonded dissimilar wedges

II. ANALYSIS METHODS

The FE model considered in this paper is shown in Fig.2 which is the same as the one of Jen[1]. Five adhesive thicknesses, i.e., 0.1, 0.2, 0.5, 1.6, 3.2mm, and three overlap lengths, i.e., 10, 16, 24mm are considered as the bonding dimensions of the specimens. The fillet angles at the ends of the adhesive considered in the FE models are 90° because the excessive adhesive fillets are assumed to be cut transversely at the ends of adherents along the edges. The geometry and

N.A.N. Author is with the Department of Mechanical Engineering, Kyushu Institute of Technology, Kitakyushu, CO 8048550 Japan (phone: 093-884-3124 fax:093-884-3124;e-mail: noda@mech.kyutech.ac.jp).

Y.Z. Author is with the Department of Mechanical Engineering, Kyushu Institute of Technology, Kitakyushu, CO 8048550 Japan (phone: 093-884-3124 fax:093-884-3124;e-mail: zyhangyu1225@yahoo.com).

T. T. Author is with the Department of Mechanical Engineering, Kyushu Institute of Technology, Kitakyushu, CO 8048550 Japan (phone: 093-884-3124 fax:093-884-3124; e-mail:j344125k@tobata.isc.kyutech.ac.jp).

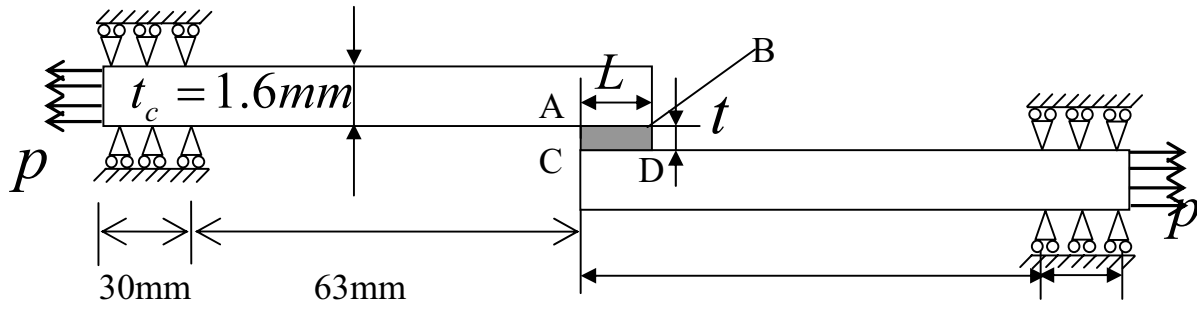


Fig.2 The geometry and boundary conditions of the single-lap joint model

boundary conditions of the model are shown in Fig.2. For the single-lap joint, the singularity stress exists at points A, B, C, D. However, it is known that singularity at point A and D is more important than the one at point B and C, because fracture often occurs around point A and D [13]. For the geometry of single-lap joint shown in Fig.2, the order of singularity λ has real roots, and in this case stresses at point A and C can be expressed by the following expressions.

$$\sigma_{\theta} = r^{\lambda-1} f_{\theta\theta}^c K_{\sigma}^o = r^{\lambda-1} K_{\sigma},$$

$$\tau_{r\theta} = r^{\lambda-1} f_{r\theta}^c K_{\tau}^o = r^{\lambda-1} K_{\tau} \quad (2)$$

The intensities of singular stress for tension and shear K_{σ}, K_{τ} are defined respectively as the followings [].

$$K_{\sigma} = \lim_{r \rightarrow 0} \left[r^{1-\lambda} \times \sigma_{\theta|\theta=\pi/2}(r) \right],$$

$$K_{\tau} = \lim_{r \rightarrow 0} \left[r^{1-\lambda} \times \tau_{r\theta|\theta=\pi/2}(r) \right] \quad (3)$$

In this paper, the finite element method is used to obtain the stress at the joint of interface, and the software is MSC. MARC 2007. Because at the end of the interface, the stress $\lim_{r \rightarrow 0} \sigma_{\theta|\theta=\pi/2}$ has singularity, that it to say that $\lim_{r \rightarrow 0} \sigma_{\theta|\theta=\pi/2}$ goes to infinity, and cannot be obtained by FEM accurately.

Therefore, the intensity of singular stress cannot be obtained by FEM easily, which means

$$K_{\sigma} = \lim_{r \rightarrow 0} \left[r^{1-\lambda} \times \sigma_{\theta|\theta=\pi/2}(r) \right] \neq \lim_{r \rightarrow 0} \left[r^{1-\lambda} \times \sigma_{\theta|\theta=\pi/2}^{FEM}(r) \right]$$

$$K_{\tau} = \lim_{r \rightarrow 0} \left[r^{1-\lambda} \times \tau_{r\theta|\theta=\pi/2}(r) \right] \neq \lim_{r \rightarrow 0} \left[r^{1-\lambda} \times \tau_{r\theta|\theta=\pi/2}^{FEM}(r) \right] \quad (4)$$

In this paper, therefore, the ratio of intensity of singular stress $K_{\sigma}^1/K_{\sigma}^2, K_{\tau}^1/K_{\tau}^2$ will be considered. Here, the superscripts 1, 2 mean specific problems whose t/t_c or overlap length L are distinct. As shown in Eq. (2), the intensity of singular stress is related to the distance r , singular index λ , and limiting stress $\lim_{r \rightarrow 0} \sigma_{\theta|\theta=\pi/2}$. Consider different thicknesses t_1, t_2 as problem 1 and problem 2, both of which have the same

stress at infinity σ and material combinations. Therefore, it should be noted that the singular index $\lambda_1 = \lambda_2$. As shown in Eq. (3), the ratios of intensity of singular stress $K_{\sigma}^1/K_{\sigma}^2$ and K_{τ}^1/K_{τ}^2 are controlled by the ratios of stress $\lim_{r \rightarrow 0} (\sigma_{\theta|\theta=\pi/2}^1 / \sigma_{\theta|\theta=\pi/2}^2)$ and $\lim_{r \rightarrow 0} (\tau_{r\theta|\theta=\pi/2}^1 / \tau_{r\theta|\theta=\pi/2}^2)$.

$$\frac{K_{\sigma}^1}{K_{\sigma}^2} = \lim_{r \rightarrow 0} \frac{\left[r^{1-\lambda_1} \sigma_{\theta|\theta=\pi/2}^1(r) \right]}{\left[r^{1-\lambda_1} \sigma_{\theta|\theta=\pi/2}^2(r) \right]} = \lim_{r \rightarrow 0} \frac{\sigma_{\theta|\theta=\pi/2}^1(r)}{\sigma_{\theta|\theta=\pi/2}^2(r)}$$

$$\frac{K_{\tau}^1}{K_{\tau}^2} = \lim_{r \rightarrow 0} \frac{\left[r^{1-\lambda_1} \tau_{r\theta|\theta=\pi/2}^1(r) \right]}{\left[r^{1-\lambda_1} \tau_{r\theta|\theta=\pi/2}^2(r) \right]} = \lim_{r \rightarrow 0} \frac{\tau_{r\theta|\theta=\pi/2}^1(r)}{\tau_{r\theta|\theta=\pi/2}^2(r)} \quad (5)$$

Therefore, in this paper, the ratio of intensity of singular stress is mainly considered in the analysis. The intensity of singular stress depends on the geometry and loading conditions for the model. To discuss the effects of geometry on the intensity of singular stress, two reference problems are used in this paper. When the effect of adhesive thickness on the intensity of singular stress is discussed, the problem when the adhesive thickness $t = t_c = 1.6mm$ and $L = 10mm$ is considered as the reference problem, and the adhesive thickness is changed as 0.1, 0.2, 0.5, 1.6, 3.2mm. When the effect of overlap length on the intensity of singular stress, the problem when $t = 0.5mm$ and $L = 16mm$ is considered as the reference problem, and the overlap length is changed as 10, 16, 24mm. To understand the effect of adhesive thickness on the intensity of singular stress σ_y and τ_{xy} , stress distributions are considered along the interface between adhesive and adherent near the point A with varying adhesive thickness. The material for the adhesive is resin whose elastic modulus equals to 2.43 GPa and Poisson's ratio equals to 0.41, and the adherent is aluminum 5052-H32 whose elastic modulus equal to 75.8 GPa and Poisson's ratio equals to 0.37. To consider the singular stress at the edge of the interface, refined meshes are used near the ends of interface. Table 1(a) shows the stress distributions σ_y on the interface near the point A with different adhesive thickness when the smallest element size

$1/3^8 = 1/6561 \text{ mm}$. From the values of stresses σ_y , obtained by FEM, it is noted that stresses should go to infinity at the end of interface, and although FEM results cannot express $\lim_{r \rightarrow 0} \sigma_{\theta|\theta=\pi/2}$ accurately. However, FEM may express $\lim_{r \rightarrow 0} (\sigma_{\theta|\theta=\pi/2}^1 / \sigma_{\theta|\theta=\pi/2}^2)$ accurately, because the ratio does not go to infinity at $r \rightarrow 0$. Therefore, (3) can be changed to the following expression.

$$\frac{K_{\sigma}^1}{K_{\sigma}^2} = \lim_{r \rightarrow 0} \frac{r^{1-\lambda_1} \sigma_{\theta|\theta=\pi/2}^1(r)}{r^{1-\lambda_1} \sigma_{\theta|\theta=\pi/2}^2(r)} = \lim_{r \rightarrow 0} \frac{\sigma_{\theta|\theta=\pi/2}^1(r)}{\sigma_{\theta|\theta=\pi/2}^2(r)} = \lim_{r \rightarrow 0} \frac{\sigma_{\theta|\theta=\pi/2}^{1,FEM}(r)}{\sigma_{\theta|\theta=\pi/2}^{2,FEM}(r)}$$

$$\frac{K_{\tau}^1}{K_{\tau}^2} = \lim_{r \rightarrow 0} \frac{r^{1-\lambda_1} \tau_{r\theta|\theta=\pi/2}^1(r)}{r^{1-\lambda_1} \tau_{r\theta|\theta=\pi/2}^2(r)} = \lim_{r \rightarrow 0} \frac{\tau_{r\theta|\theta=\pi/2}^1(r)}{\tau_{r\theta|\theta=\pi/2}^2(r)} = \lim_{r \rightarrow 0} \frac{\tau_{r\theta|\theta=\pi/2}^{1,FEM}(r)}{\tau_{r\theta|\theta=\pi/2}^{2,FEM}(r)} \tag{6}$$

In Table I (a) the ratio of stress $\sigma_y / \sigma_{y|t/t_c=1}$ is indicated in the parentheses. It is found that the ratio is almost constant by 4 digit independent of r . Table 1 (b) shows τ_{xy} stress distributions and the ratio $\tau_y / \tau_{xy|t/t_c=1}$ for the problem $t = t_c = 16 \text{ mm}$ and $L = 100 \text{ mm}$ considered as the reference problem. It is found that although the FEM cannot give the exact values of stress at the end of interface, the ratio $\tau_y / \tau_{xy|t/t_c=1}$ is almost constant independent of r . Also, it is found that the ratio of $\sigma_y / \sigma_{y|t/t_c=1}$ and $\tau_y / \tau_{xy|t/t_c=1}$ is almost the same.

Table II(a) shows the results for σ_y and the ratio $\sigma_y / \sigma_{y|t/t_c=1}$ with the smallest mesh size $1/3^4 = 1/81 \text{ mm}$. In this case, it is found that the ratios are almost constant by 3 digit independent of r . It is also found that the ratio in Table 1(a) and Table 2 (a) coincide each other by 3 digit. Although real interface singular stresses cannot be expressed easily by using the FEM because the values of stress largely depend on the mesh size, it is found that the ratio of stress can be obtained vary accurately as shown in Table 1 and Table 2. In other words, the ratio of interface stress is nearly independent of mesh size. Table 2 (b) shows the results for τ_{xy} and the ratio $\tau_y / \tau_{xy|t/t_c=1}$ with the smallest mesh size $1/3^4 = 1/81 \text{ mm}$. In this case, it is also found that the ratios are almost constant by 3 digit independent of r , and the ratio in Table 1(b) and Table 2 (b) coincide each other by 3 digit. Therefore, for the stress τ_{xy} , it also can be said that the ratio of interface stress is nearly independent of mesh size. Moreover, the ratios of σ_y and τ_{xy} are almost the same independent of mesh size. As explained above, the ratio $K_{\sigma}^1 / K_{\sigma}^2$ and K_{τ}^1 / K_{τ}^2 are controlled respectively by the ratio of stress $\lim_{r \rightarrow 0} (\sigma_{\theta|\theta=\pi/2}^1 / \sigma_{\theta|\theta=\pi/2}^2)$ and $\lim_{r \rightarrow 0} (\tau_{r\theta|\theta=\pi/2}^1 / \tau_{r\theta|\theta=\pi/2}^2)$ along r , and as shown in Table 1 and Table 2 since the ratio of σ_y^1 / σ_y^2 and $\tau_{xy}^1 / \tau_{xy}^2$ are the same, only the ratio σ_y^1 / σ_y^2 is enough to discuss the ratio $K_{\sigma}^1 / K_{\sigma}^2$ and K_{τ}^1 / K_{τ}^2 , and the ratio

TABLE I
STRESS DISTRIBUTION ALONG THE INTERFACE WITH THE SMALLEST MESH SIZE $1/3^8 = 1/6561 \text{ mm}$ WHEN ALUMINUM 5052-H32 AND RESIN ARE CONSIDERED AS ADHERENT AND ADHESIVE RESPECTIVELY. THE RATIO OF STRESS DISTRIBUTIONS ARE INDICATED IN PARENTHESES

(a) σ_y and $(\sigma_y / \sigma_{y|t/t_c=1})$ obtained with the smallest mesh size $1/3^8 = 1/6561 \text{ mm}$ and $L = 10 \text{ mm}$

t/t_c r/L	1/16	2/16	5/16	16/16	32/16
$\rightarrow 0$	36.874(0.706)	36.046(0.690)	38.205(0.731)	52.254(1.000)	71.580(1.370)
1/65610	23.123(0.706)	22.600(0.690)	23.949(0.731)	32.752(1.000)	44.856(1.370)
2/65610	17.415(0.706)	17.021(0.690)	18.035(0.731)	24.663(1.000)	33.774(1.369)
3/65610	14.403(0.706)	14.073(0.690)	14.909(0.731)	20.388(1.000)	27.918(1.369)
4/65610	12.561(0.707)	12.272(0.690)	13.000(0.731)	17.776(1.000)	24.339(1.369)
5/65610	11.389(0.707)	11.126(0.690)	11.785(0.731)	16.114(1.000)	22.062(1.369)
6/65610	10.542(0.707)	10.298(0.691)	10.907(0.731)	14.913(1.000)	20.417(1.369)
7/65610	9.895(0.707)	9.666(0.691)	10.237(0.731)	13.996(1.000)	19.161(1.369)
8/65610	9.379(0.707)	9.161(0.691)	9.701(0.731)	13.264(1.000)	18.157(1.369)
9/65610	8.953(0.707)	8.744(0.691)	9.260(0.731)	12.669(1.000)	17.330(1.369)

(b) τ_{xy} and $(\tau_{xy}/\tau_{xy/t/t_c=1})$ obtained with the smallest mesh size $1/3^8 = 1/6561mm$ and $L = 10mm$

$r/L \backslash t/t_c$	1/16	2/16	5/16	16/16	32/16
$\rightarrow 0$	-11.921(0.706)	-11.654(0.690)	-12.352(0.731)	-16.894(1.000)	-23.144(1.370)
1/65610	-6.889(0.706)	-6.735(0.690)	-7.138(0.731)	-9.764(1.000)	-13.375(1.370)
2/65610	-5.559(0.705)	-5.435(0.690)	-5.761(0.731)	-7.880(1.000)	-10.797(1.370)
3/65610	-5.077(0.705)	-4.964(0.690)	-5.262(0.731)	-7.196(1.000)	-9.859(1.370)
4/65610	-4.671(0.705)	-4.567(0.690)	-4.841(0.731)	-6.621(1.000)	-9.072(1.370)
5/65610	-4.375(0.705)	-4.278(0.690)	-4.536(0.731)	-6.203(1.000)	-8.498(1.370)
6/65610	-4.135(0.705)	-4.044(0.691)	-4.287(0.731)	-5.864(1.000)	-8.033(1.370)
7/65610	-3.938(0.705)	-3.852(0.691)	-4.084(0.731)	-5.586(1.000)	-7.653(1.370)
8/65610	-3.774(0.705)	-3.691(0.691)	-3.914(0.731)	-5.353(1.000)	-7.334(1.370)
9/65610	-3.635(0.705)	-3.556(0.691)	-3.770(0.731)	-5.156(1.000)	-7.064(1.370)

TABLE II

STRESS DISTRIBUTION ALONG THE INTERFACE WITH THE SMALLEST MESH SIZE $1/3^4 = 1/81mm$ WHEN ALUMINUM 5052-H32 AND RESIN ARE CONSIDERED AS ADHERENT AND ADHESIVE RESPECTIVELY . THE RATIO OF STRESS DISTRIBUTIONS ARE INDICATED IN PARENTHESES

(a) σ_y and $(\sigma_y/\sigma_{y/t/t_c=1})$ obtained with the smallest mesh size $1/3^4 = 1/81mm$ and $L = 10mm$

$r/L \backslash t/t_c$	1/16	2/16	5/16	16/16	32/16
$\rightarrow 0$	11.028(0.707)	10.771(0.690)	11.410(0.731)	15.603(1.000)	21.367(1.369)
1/810	6.846(0.708)	6.687(0.692)	7.076(0.732)	9.670(1.000)	13.233(1.368)
2/810	5.119(0.707)	5.007(0.692)	5.299(0.732)	7.239(1.000)	9.901(1.368)
3/810	4.200(0.705)	4.118(0.692)	4.360(0.732)	5.954(1.000)	8.141(1.367)
4/810	3.635(0.703)	3.573(0.691)	3.786(0.732)	5.170(1.000)	7.067(1.367)
5/810	3.272(0.700)	3.225(0.690)	3.421(0.732)	4.672(1.000)	6.384(1.367)
6/810	3.007(0.697)	2.972(0.689)	3.157(0.732)	4.312(1.000)	5.891(1.366)
7/810	2.803(0.694)	2.779(0.688)	2.955(0.732)	4.037(1.000)	5.515(1.366)
8/810	2.639(0.691)	2.623(0.687)	2.794(0.732)	3.818(1.000)	5.214(1.366)
9/810	2.503(0.688)	2.494(0.686)	2.661(0.732)	3.637(1.000)	4.966(1.366)

$\lim_{r \rightarrow 0} (\sigma^1_{\theta|\theta=\pi/2} / \sigma^2_{\theta|\theta=\pi/2})$ along r is independent of r , only the stress σ_y at the first element can be considered.

When the effect of overlap length on the intensity of singular stress is discussed, the results for Table 1 and Table 2 can be obtained. Therefore, it is also found that only the

stress σ_y of the first element is enough to discuss the ratio K^1_σ / K^2_σ and K^1_τ / K^2_τ .

In the following of this paper, effects of adhesive thickness and overlap length on the intensity of singular stress will be discussed using the method explained the above.

(b) τ_{xy} and $(\tau_{xy}/\tau_{xy/t/t_c=1})$ obtained with the smallest mesh size $1/3^4 = 1/81mm$ and $L = 10mm$

$r/L \backslash t/t_c$	1/16	2/16	5/16	16/16	32/16
$\rightarrow 0$	-3.490(0.706)	-3.570(0.689)	-3.699(0.731)	-5.059(1.000)	-6.929(1.370)
1/810	-2.017(0.703)	-2.060(0.689)	-2.140(0.731)	-2.928(1.000)	-4.010(1.370)
2/810	-1.629(0.701)	-1.662(0.687)	-1.731(0.730)	-2.370(1.000)	-3.247(1.370)
3/810	-1.487(0.701)	-1.517(0.687)	-1.581(0.730)	-2.166(1.000)	-2.967(1.370)
4/810	-1.367(0.700)	-1.396(0.686)	-1.454(0.730)	-1.993(1.000)	-2.731(1.370)
5/810	-1.280(0.701)	-1.308(0.685)	-1.362(0.729)	-1.867(1.000)	-2.559(1.370)
6/810	-1.209(0.702)	-1.238(0.685)	-1.287(0.729)	-1.765(1.000)	-2.419(1.371)
7/810	-1.152(0.703)	-1.182(0.685)	-1.225(0.729)	-1.681(1.000)	-2.305(1.371)
8/810	-1.104(0.704)	-1.135(0.685)	-1.174(0.729)	-1.611(1.000)	-2.209(1.371)
9/810	-1.063(0.706)	-1.096(0.685)	-1.130(0.728)	-1.552(1.000)	-2.128(1.371)

III. RESULT AND D DISCUSSION

		Material	Elastic Modulus/GPa	Poisson Ratio
Adherent	1	SUS304 (stainless steel)	206	0.3
	2	Silicon	166	0.26
	3	Aluminum 5052-H32	75.8	0.37
	4	FR-4.5 (IC substrate)	15.34	0.15
Adhesive		Resin	2.43	0.41

TABLE III MATERIAL PROPERTIES

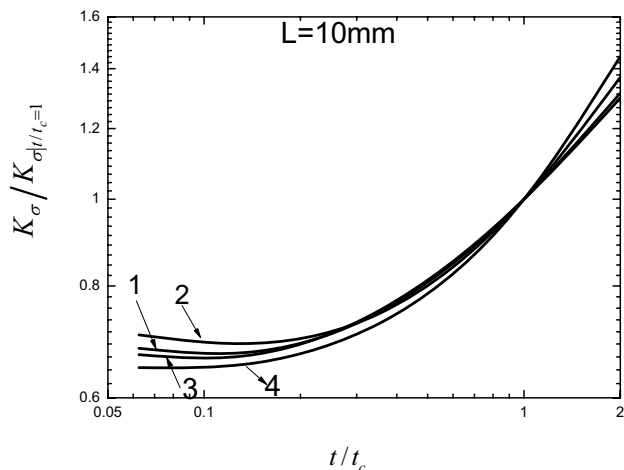
To investigate the effects of adhesive thickness and overlap length on the intensity of singular stresses, aluminum 5052-H32, SUS304 (stainless steel), silicon and IC substrate FR-4.5 are considered for the adherents, and resin is considered for the adhesive. Table 3 shows the material properties of adherents and adhesive. Here, E, ν are the Young's modulus and the Poisson ratio of the adherent. From material 1 to material 4, the ratio of elastic modulus E_1/E_2 between adherent and adhesive decreases. Here, subscripts 1 and 2 represent adherent and adhesive respectively.

Fig.3(a) shows the relationship between the ratio $K_\sigma/K_{\sigma/t/t_c=1}$ and adhesive thickness t/t_c for material combinations 1,2, 3 and 4 when the overlap length $L = 10mm$.

It is seen that the ratio $K_\sigma/K_{\sigma/t/t_c=1}$ decreases with decreasing adhesive thickness t/t_c for all material combinations, and those values do not change very much independent on material combinations.

Fig.3 (b) shows the relationship between the ratio $K_\sigma/K_{\sigma/t/t_c=1}$ and adhesive thickness t/t_c for material combinations 1,2, 3 and 4 when the overlap length $L = 16mm$. Comparing with the case when $L = 10mm$, the ratio $K_\sigma/K_{\sigma/t/t_c=1}$ also decreases with decreasing adhesive thickness t/t_c for all material combinations. The values are almost the same for the material combinations 1,2 and 3.

Fig.4 shows the relationship between the ratio $K_\sigma/K_{\sigma/L=16}$ and overlap length $L/16mm$ for material combinations 1,2, 3 and 4 when the adhesive thickness $t = 0.5mm$. Here, the problem when $L = 16mm$ is considered as the reference problem. The ratio $K_\sigma/K_{\sigma/L=16}$ decreases with increasing the overlap length, and the decrements depending on material combinations.



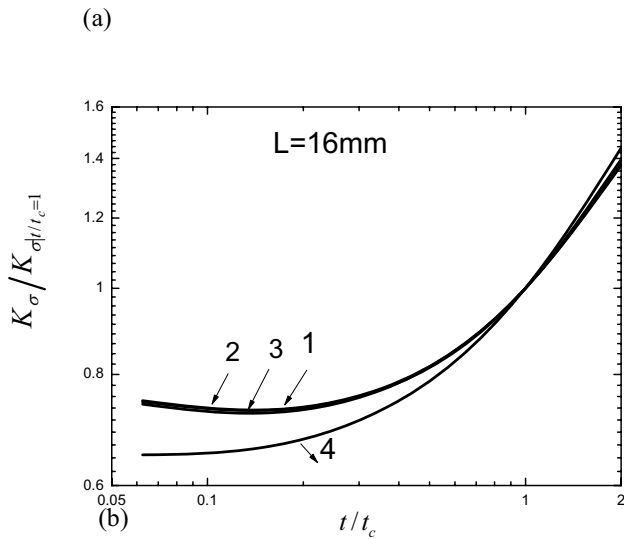


Fig.3 The relationship between the ratio $K_{\sigma}/K_{\sigma|t/t_c=1}$ and the adhesive thickness t/t_c (a) $L = 10mm$; (b) $L = 16mm$

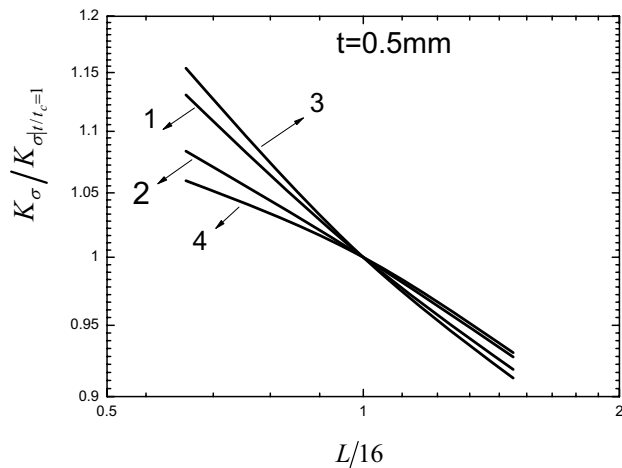


Fig.4 The relationship between the ratio $K_{\sigma}/K_{\sigma|t/t_c=1}$ and the overlap length $L/16$ when $t = 0.5mm$

IV. CONCLUSIONS

In this paper, the strength of single-lap joint was evaluated on the basis of intensity of singular stress by the FEM, and a useful method was proposed using the stress of first element at the end of the interface. The conclusions of this paper are in the followings.(1) Since the real interface stress goes to infinity at the end, FEM cannot express the stress accurately. However, it

is found that the ratios of intensity of singular stress $K_{\sigma}^1/K_{\sigma}^2$ and K_{τ}^1/K_{τ}^2 can be determined accurately from FEM results $\lim_{r \rightarrow 0} (\tau_{r\theta|\theta=\pi/2}^{1,FEM} / \tau_{r\theta|\theta=\pi/2}^{2,FEM})$, $\lim_{r \rightarrow 0} (\sigma_{r\theta|\theta=\pi/2}^{1,FEM} / \sigma_{r\theta|\theta=\pi/2}^{2,FEM})$ respectively. FEM can express the values of the ratio accurately independent of FEM mesh size.

(2) About the effect of adhesive thickness on the intensity of singular stress, it is found that the ratio $K_{\sigma}/K_{\sigma|t/t_c=1}$ decreases with decreasing adhesive thickness t/t_c for material combinations 1,2, 3 and 4 , and the results are different when the overlap length is different. About the effect of overlap length on the intensity of singular stress, it is found the ratio $K_{\sigma}/K_{\sigma|t/t_c=1}$ decreases with increasing overlap length for material combinations 1,2, 3 and 4 .

REFERENCES

- [1] Y.M. Jen, , C.W. Ko, "Evaluations of fatigue life of adhesively bonded aluminum single-lap joint using interfacial parameters", *International Journal of Fatigue*, 32, pp.330-340,2010.
- [2] G. Li, P. Lee-Sullivan, R.W. Thring, "Nolinear finite element analysis of stress and strain distributions across the adhesive thickness in composite single-lap joint", *Composite Structures*,46, pp.395-403, 1999.
- [3] K.J. Lalit, Y.W. Mai, "Analysis of resin-transfer-moulded single-lap joints", *Composites Science and Technology*, 59, pp.1513-1518, 1999.
- [4] Z.M. Yan, M. You, X.S. Yi, X.L. Zheng, Z. Li, "A numerical study of parallel slot in adherend on the stress distribution in adhesively bonded aluminum single lap joint", *International Journal of Adhesion & Adhesives*, 27, pp.687-695, 2007.
- [5] S.A.Hashim,"Strength of resin-coated-adhesive-bonded doublelap-shear ultrasonic joints at ambient temperature", *International Journal of Adhesion & Adhesives*, 29, pp.294-301, 2009.
- [6] R. Yuuki, *Mechanics of interface*, Baifuukan, 1993 (in Japanese).
- [7] D.H.Chen, H.Nisitani, "Singular stress field in two bonded wedges", *The Japan Society of Mechanical Engineers*, vol.58, no.547 pp.457-464, 1992.
- [8] D. Munz, Y.Y. Yang, "Stresses near the edge of bonded dissimilar materials described by two stress intensity factors", *International Journal of Fracture*, 60, pp. 169-177, 1993.
- [9] M. Imanakaa, K. Ishiib, H. Nakayamac, "Evaluation of fatigue strength of adhesively bonded single and single step double lap joints based on stress singularity parameters", *Engineering Fracture Mechanics*, 62, pp.409-424, 1999.
- [10] T. Hattori, S. Sakata, T. Hatsuda, G. Murakami, "A stress singularity parameter approach for evaluating adhesive strength", *The Japan Society of Mechanical Engineers*, 31, pp.718-723,1988.
- [11] T. Hattori. "A stress-singularity-parameter approach for evaluating the adhesive strength of single-lap joints", *The Japan Society of Mechanical Engineers*, 34, pp.326-331, 1991.
- [12] A. Barroso, V. Mantic, F. Paris , "Singularity parameter determination in adhesively bonded lap joints for use in failure criteria", *Composites Science and Technology*, 68, pp.2671-2677, 2008.
- [13] P.N.B. Reis, F.J.V. Antunes, J.A.M. Ferreira, "Influence of superposition length on mechanical resistance of single-lap adhesive joints", *Composite Structures*, 67, pp.125-133, 2005.